Report on Spectrometer Offsets

Rikki E. Roché

last updated February 6, 2001

The determination of the mis-pointing of the Hall A High Resolution Spectrometers, both electron (HRSe) and hadron (HRSh), is accomplished using two different methods: (1) using a carbon pointing run and (2) using a script, called LVDT, to determine the offsets from the EPICS data in the CODA file.

For the carbon pointing runs the spectrometer mis-pointing was found using equation (1):

$$p = -y_{tg} - z_{tg} \sin\theta + beamx \cos\theta, \tag{1}$$

where y_{tg} is the non-dispersive position at the scattering point of the target, z_{tg} is the position at the scattering point in the target along the beam (this value comes from a survey of the target and is shown in table 1), $beamx$ is the beam

survey date	z_{tg} (mm)	run numbers
May 16, 2000	1.01±0.5	1025-1340
May 26, 2000	0.46±0.5	1346-2688
June 30, 2000	1.14±0.5	2720-4040

Table 1: Survey z_{tg} positions.

position at $z = 0$ derived from the bpm positions, and θ is the spectrometer angle. For the HRSe θ is entered as a positive value while HRSh angles are entered as negative values. Values for y_{tg} and $beamx$ were determined from histogram fits using some initial x and z offset values in the ESPACE header file. Examples of the y_{tg} and $beamx$ fits are shown in figures 1 and 2. The mis-pointing for each spectrometer arm is then calculated using equation (1), the y_{tg} value found from the paw fit, the z_{tg} survey position shown in table 1, the $beamx$ position found from the paw fit, and the spectrometer angle. From the mis-pointing and spectrometer angle, the spectrometer offsets in the x and z directions are determined by:

$$x = p\cos\theta \tag{2}$$
$$z = -p\sin\theta. \tag{3}$$

The carbon mis-pointing and offset values found were then compared to values found from running the LVDT. This script takes the spectrometer angle floor mark and vernier, combined with the CODA data file and determines the spectrometer mis-pointing and offsets.

Comparisons of the mis-pointing and spectrometer x and z offsets for each spectrometer are shown in the following figures. Figure 4 shows the electron spectrometer mis-pointing, and figures 5 and 6 show the electron x- and z-offsets, where the shaded regions correspond to the survey values. Figure 7 shows the comparison of the hadron arm spectrometer mis-pointing, and figures

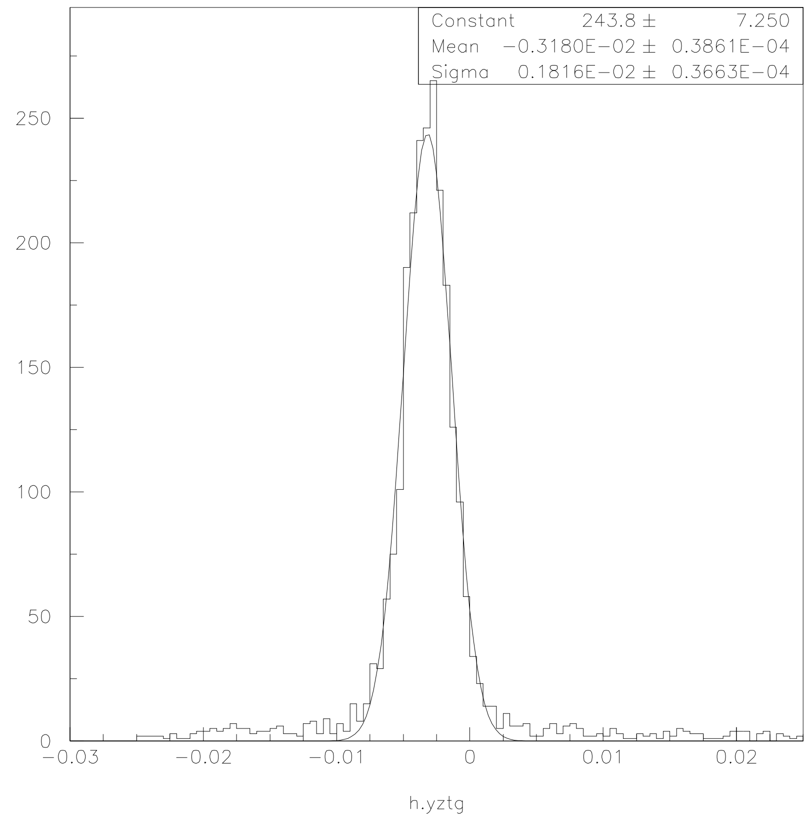

Figure 1: Example of a plot of y_{tg} from paw hbook (run 1216).

8 and 9 show the comparisons of the x- and z-offsets, where the shaded regions represent offsets determined by spectrometer surveys. As you can see, both the mis-pointing values and the spectrometer offsets for the carbon pointing method, the LVDT method, and the surveys for the HRSe agree very well, but not so for the HRSh.

To determine which set of detector offsets, those found using the carbon pointing method versus those found from the LVDT calculation, should be used in the ESPACE header files for further analysis, ESPACE was rerun for each set of offsets. The *reactz* variable, the z-coordinate of the reaction point in the target, was determined by a histogram fit. An example of this *reactz* variable determination is shown in figure 3. This *reactz* should be the same as the survey value for z_{tg}. Figures 10 and show the *reactz* determined using the offsets found for both methods. The shaded region again represents the survey results and

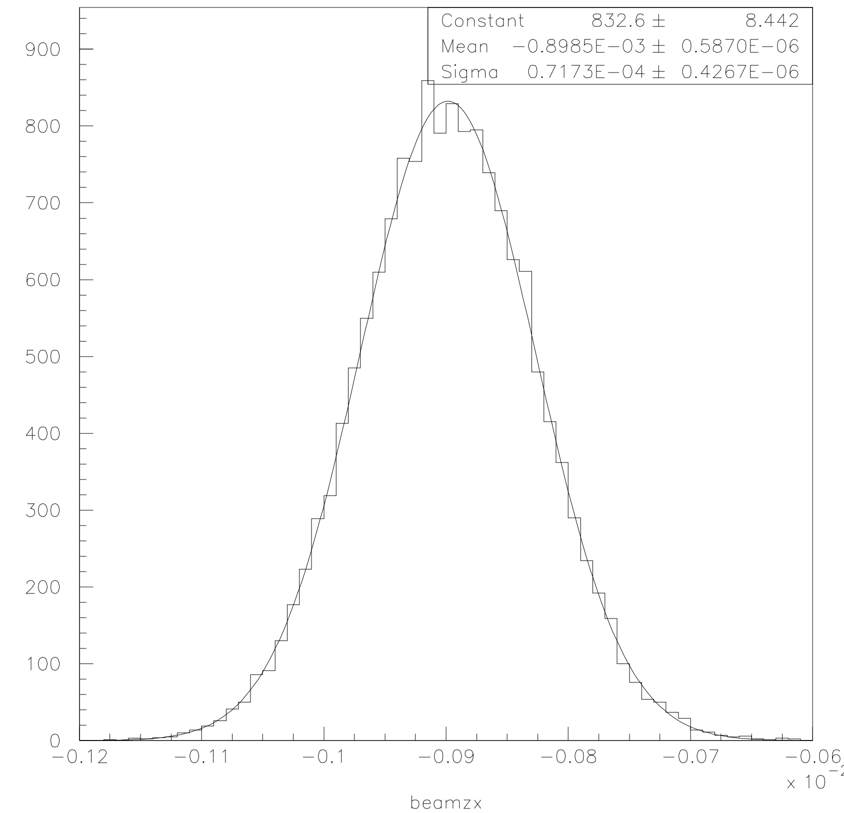

Figure 2: Example of a plot of *beamx* from paw hbook (run 1216).

the associated errors. In both of these figures, it seems the spectrometer offsets found using the carbon pointing runs reproduces the z_{tg} position much better than the spectrometer offsets found using the LVDT script. Figure 12 shows the differences between the reactz position found in the electron and hadron arm analyses. You can see from this plot that the carbon pointing method gives consistent results for reactz from both spectrometer arms, while not so for the LVDT method. Run number 1760 was used to optimize the HRSe detector offsets used in the analysis database while run 2722 was used to optimize the offsets for the HRSh. The spectrometer offsets found using the carbon pointing method should therefore be used in further $\mathrm{N} \rightarrow \Delta$ analysis.

In conclusion, the carbon pointing method spectrometer offsets will be used in the header files for analysis.

Table 2 lists the values for the electron and hadron arm mis-pointing for the

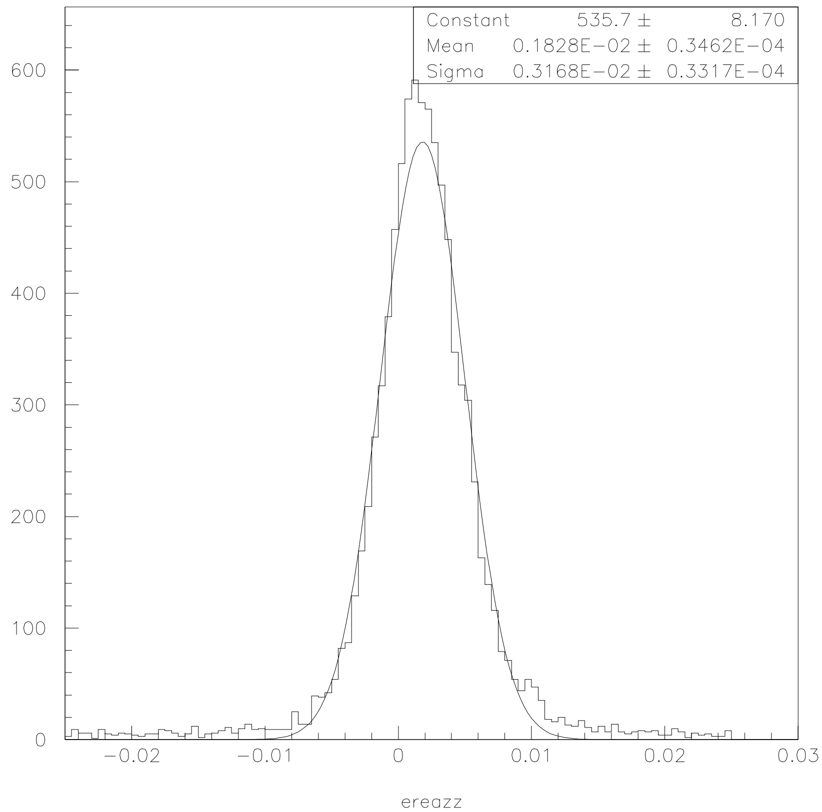

Figure 3: Example of a plot of *reactz* from paw hbook (run 1216).

carbon pointing method, the LVDT method, and the survey values. Tables 3 and 4 give the x- and z-offsets for the HRSe and HRSh. Table 5 lists the *reactz* position determined by both methods compared to survey.

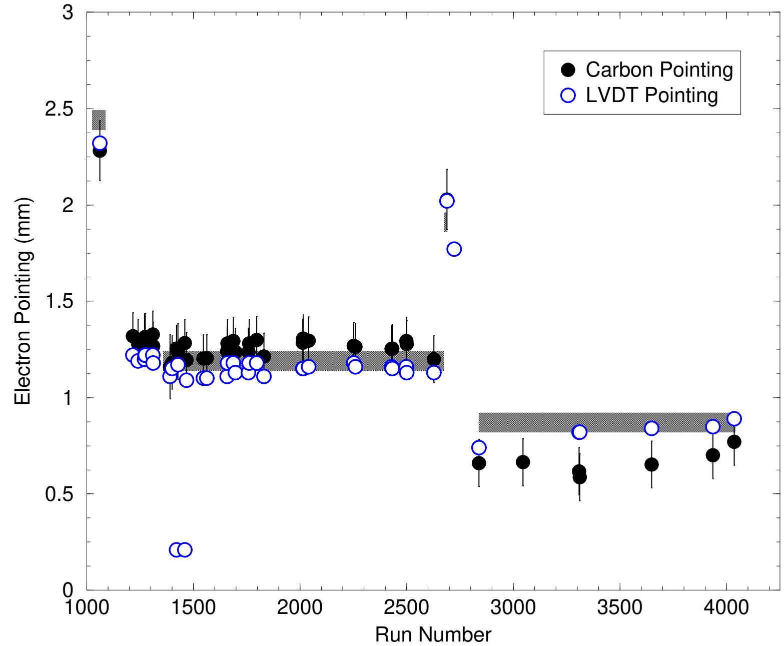

Figure 4: Electron arm spectrometer mis-pointing.

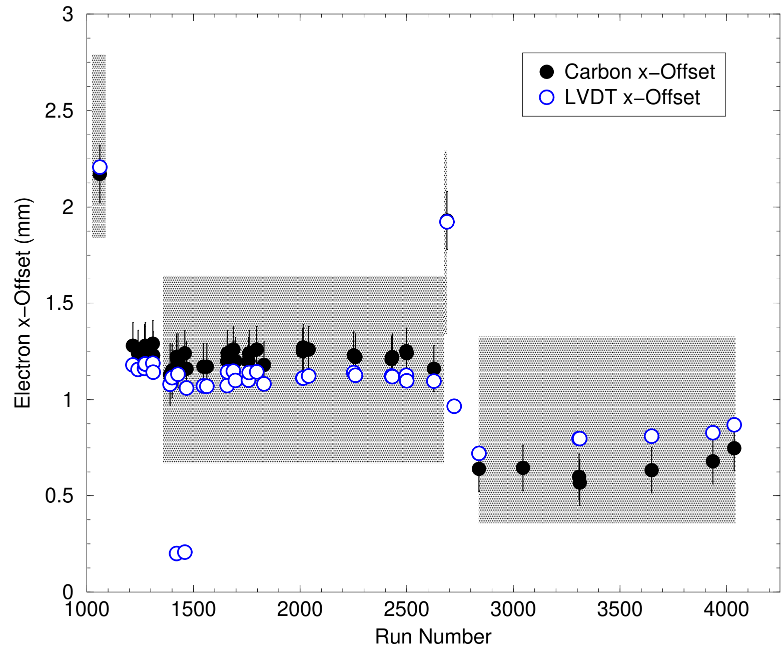

Figure 5: Electron arm x-offsets.

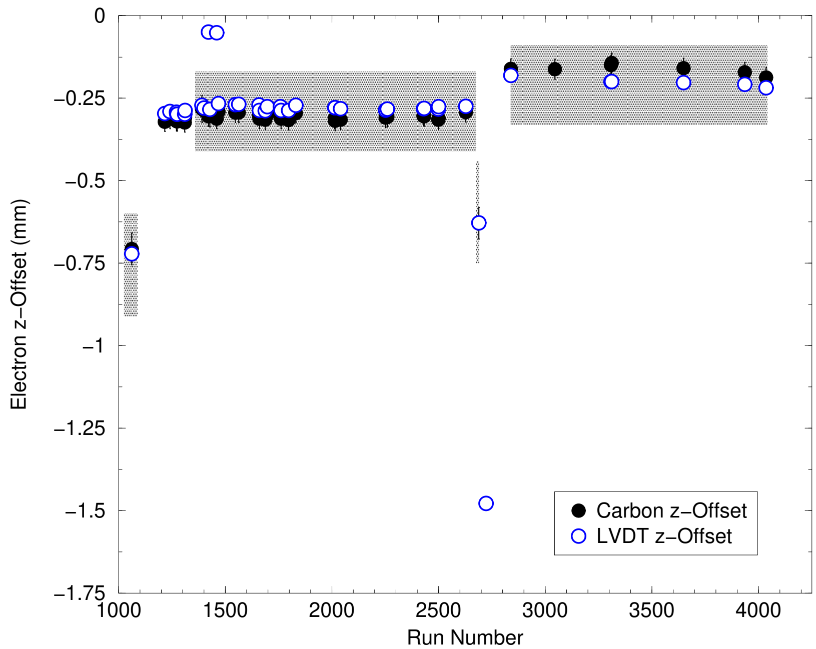

Figure 6: Electron arm z-offsets.

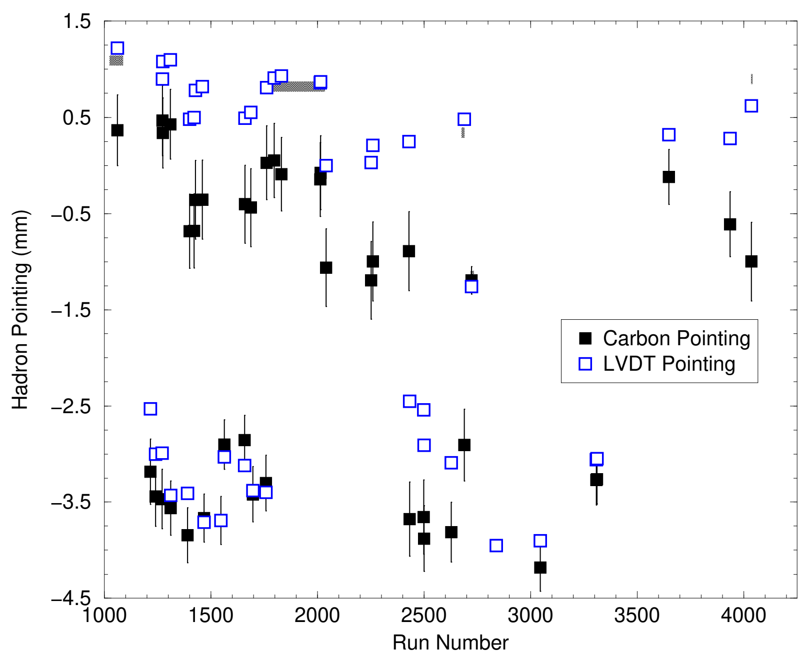

Figure 7: Hadron arm spectrometer mis-pointing.

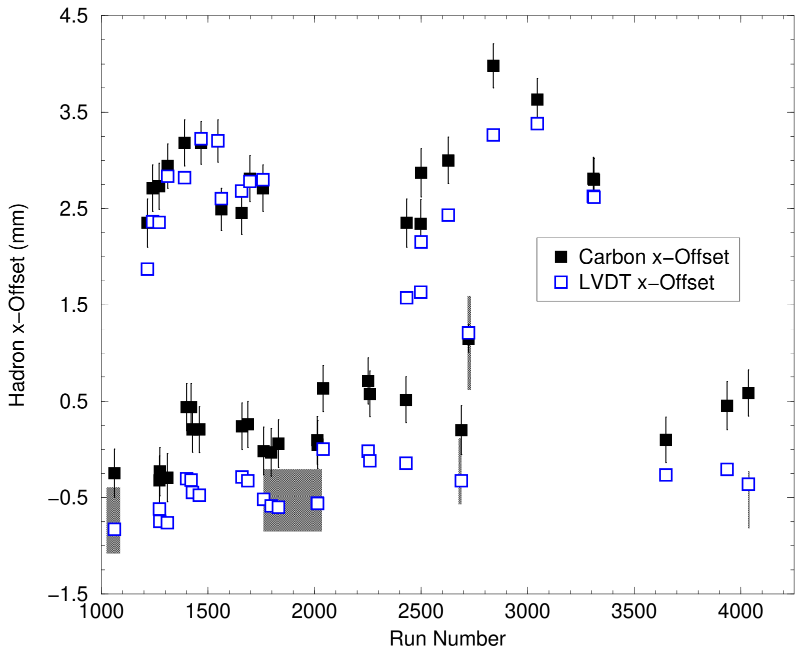

Figure 8: Hadron arm x-offsets.

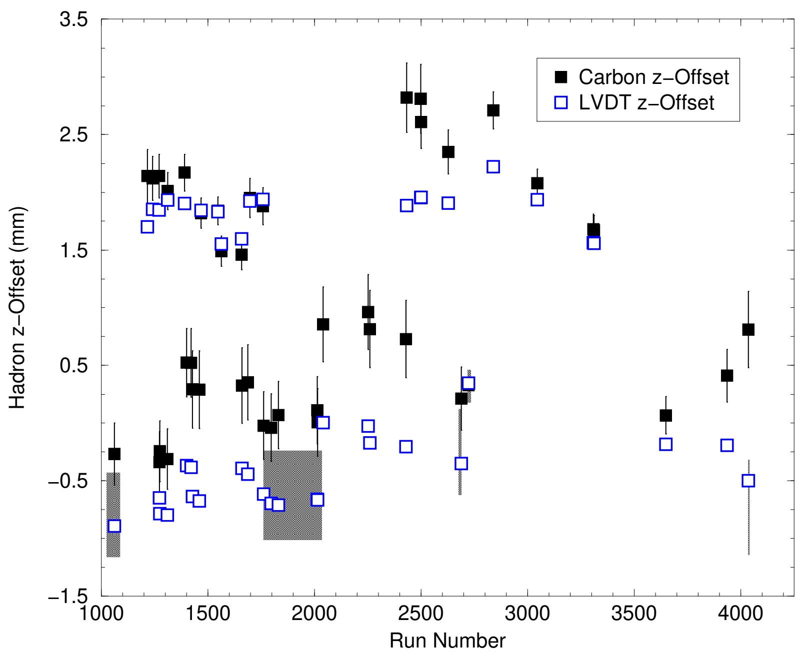

Figure 9: Hadron arm z-offsets.

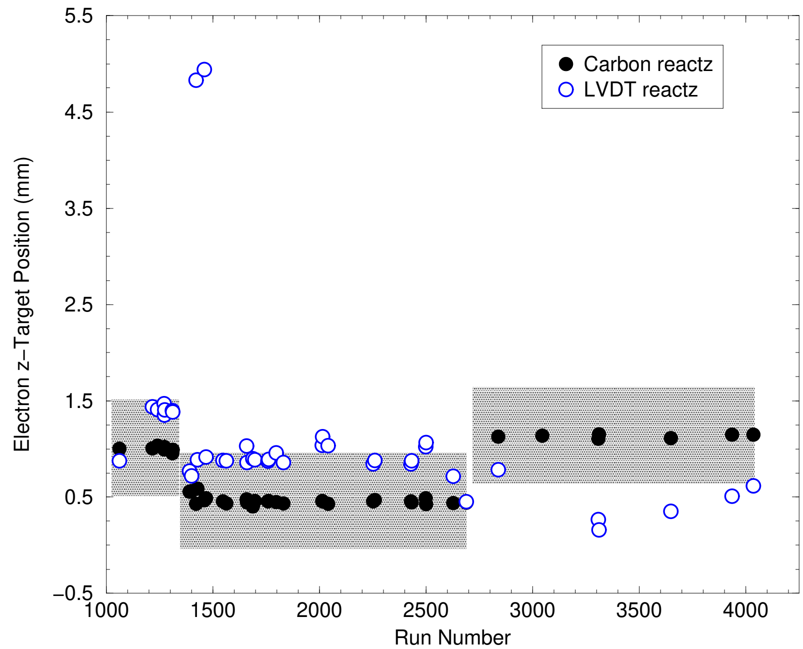

Figure 10: Electron arm reactz positions.

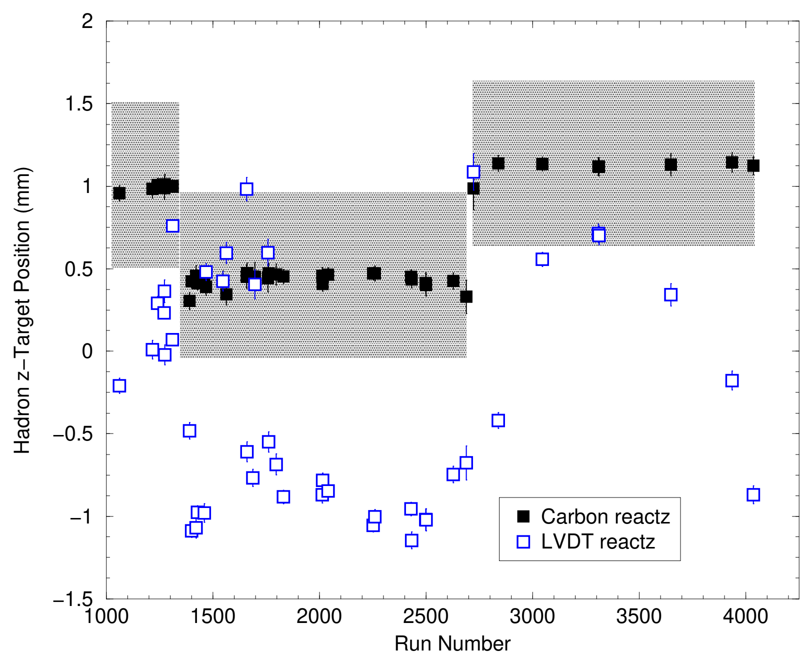

Figure 11: Hadron arm reactz positions.

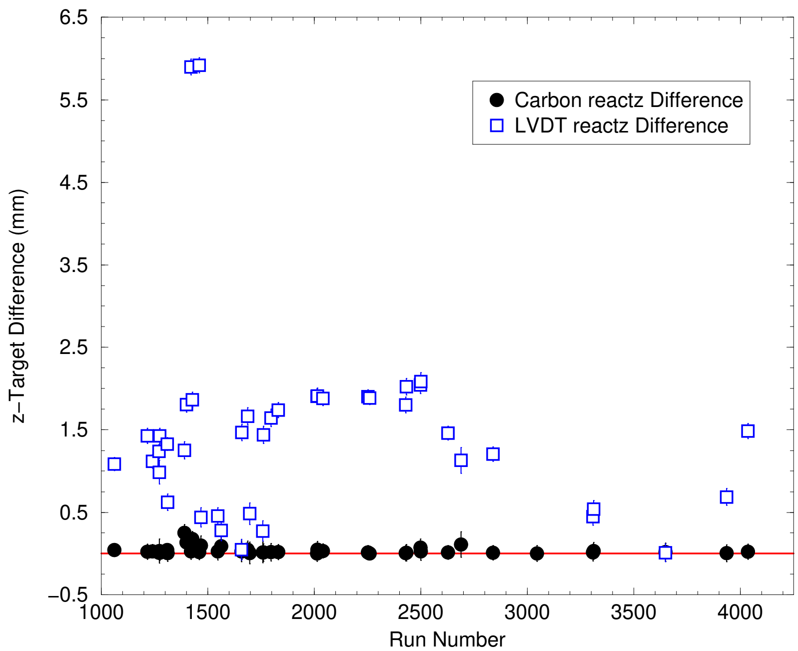

Figure 12: Difference between electron and hadron arm reactz positions.

θ_{cm}	run	electron carbon	electron LVDT	electron survey	hadron carbon	hadron LVDT	hadron survey
	1061	2.281±0.155	2.32	2.44±0.50	0.365±0.368	1.22	1.09±0.50
0°	1216	1.318±0.122	1.22	-	-3.183±0.339	-2.53	-
25°	1240	1.282±0.122	1.19	-	-3.442±0.310	-3.00	-
25°	1271	1.312±0.122	1.20	-	-3.468±0.309	-2.99	-
-25°	1273	1.300±0.123	1.22	-	0.466±0.365	0.90	-
-25°	1274	1.315±0.122	1.22	-	0.336±0.364	1.08	-
-25°	1310	1.327±0.122	1.22	-	0.428±0.363	1.10	-
50°	1311	1.267±0.123	1.18	-	-3.563±0.282	-3.43	-
50°	1390	1.160±0.167	1.11	1.19±0.50	-3.845±0.285	-3.41	-
-50°	1399	1.182±0.139	1.15	1.19±0.50	-0.683±0.386	0.48	-
-50°	1420	1.254±0.122	0.21	1.19±0.50	-0.680±0.387	1.50	-
-90°	1427	1.239±0.146	1.17	1.19±0.50	-0.358±0.410	0.78	-
-90°	1459	1.283±0.122	0.21	1.19±0.50	-0.355±0.411	0.82	-
90°	1467	1.195±0.144	1.09	1.19±0.50	-3.666±0.251	-3.71	-
90°	1547	1.203±0.122	1.10	1.19±0.50	-3.692±0.250	-3.69	-
135°	1562	1.204±0.123	1.10	1.19±0.50	-2.902±0.258	-3.03	-
135°	1658	1.240±0.122	1.11	1.19±0.50	-2.856±0.259	-3.12	-
-135°	1660	1.282±0.122	1.18	1.19±0.50	-0.403±0.406	0.49	-
-135°	1687	1.294±0.122	1.18	1.19±0.50	-0.439±0.405	0.55	-
155°	1696	1.237±0.122	1.13	1.19±0.50	-3.418±0.289	-3.38	-
155°	1758	1.237±0.122	1.13	1.19±0.50	-3.303±0.289	-3.40	-
-155°	1761	1.282±0.122	1.18	1.19±0.50	0.027±0.384	0.81	0.82±0.50
-155°	1796	1.300±0.122	1.18	1.19±0.50	0.052±0.385	0.91	0.82±0.50
-155°	1831	1.213±0.122	1.11	1.19±0.50	-0.090±0.383	0.93	0.82±0.50
-155°	2012	1.285±0.122	1.15	1.19±0.50	-0.146±0.383	0.86	0.82±0.50
-155°	2014	1.307±0.122	1.15	1.19±0.50	-0.075±0.383	0.87	0.82±0.50
-135°	2041	1.296±0.122	1.16	1.19±0.50	-1.062±0.404	0.00	-
-135°	2252	1.269±0.122	1.18	1.19±0.50	-1.195±0.404	0.03	-
-90°	2260	1.263±0.122	1.16	1.19±0.50	-0.997±0.410	0.21	-
-90°	2429	1.252±0.122	1.16	1.19±0.50	-0.891±0.410	0.25	-
-50°	2432	1.255±0.122	1.15	1.19±0.50	-3.676±0.386	-2.45	-
-50°	2498	1.294±0.122	1.16	1.19±0.50	-3.655±0.387	-2.54	-
0°	2500	1.277±0.122	1.13	1.19±0.50	-3.879±0.340	-2.91	-
25°	2628	1.199±0.122	1.13	1.19±0.50	-3.812±0.310	-3.09	-
	2688	2.028±0.156	2.02	1.91±0.50	-2.907±0.373	0.48	0.34±0.50
	2722	-	1.77	-	-1.194±0.143	-1.26	-1.15±0.50
50°	2838	0.660±0.122	0.74	0.87±0.50	-4.813±0.283	-3.95	-
90°	3046	0.665±0.122	-	0.87±0.50	-4.179±0.249	-3.90	-
135°	3308	0.618±0.122	0.82	0.87±0.50	-3.271±0.258	-3.06	-
135°	3311	0.587±0.122	0.82	0.87±0.50	-3.262±0.258	-3.05	-
155°	3648	0.653±0.122	0.84	0.87±0.50	-0.120±0.285	0.32	-
180°	3936	0.701±0.122	0.85	0.87±0.50	-0.611±0.339	0.28	-
	4035	0.770±0.122	0.89	0.87±0.50	-1.000±0.408	0.62	0.90±0.50

Table 2: Electron and hadron arm mis-pointing (mm).

θ_{cm}	run	carbon x	LVDT x	survey x	carbon z	LVDT z	survey z
	1061	2.17±0.15	2.207	2.32±0.48	-0.707±0.048	-0.721	-0.76±0.16
0°	1216	1.28±0.12	1.180	-	-0.321±0.030	-0.296	-
25°	1240	1.24±0.12	1.156	-	-0.312±0.030	-0.721	-
25°	1271	1.27±0.12	1.162	-	-0.319±0.030	-0.292	-
-25°	1273	1.26±0.12	1.185	-	-0.316±0.030	-0.298	-
-25°	1274	1.28±0.12	1.185	-	-0.320±0.030	-0.298	-
-25°	1310	1.29±0.12	1.188	-	-0.323±0.030	-0.298	-
50°	1311	1.23±0.12	1.142	-	-0.308±0.030	-0.287	-
50°	1390	1.13±0.16	1.079	1.15±0.49	-0.282±0.041	-0.271	-0.29±0.12
-50°	1399	1.15±0.14	1.114	1.15±0.49	-0.287±0.034	-0.280	-0.29±0.12
-50°	1420	1.22±0.12	0.201	1.15±0.49	-0.305±0.030	-0.050	-0.29±0.12
-90°	1427	1.20±0.14	1.132	1.15±0.49	-0.301±0.036	-0.284	-0.29±0.12
-90°	1459	1.24±0.12	0.208	1.15±0.49	-0.312±0.030	-0.052	-0.29±0.12
90°	1467	1.16±0.14	1.059	1.15±0.49	-0.291±0.035	-0.266	-0.29±0.12
90°	1547	1.17±0.12	1.070	1.15±0.49	-0.293±0.030	-0.269	-0.29±0.12
135°	1562	1.17±0.12	1.068	1.15±0.49	-0.293±0.030	-0.268	-0.29±0.12
135°	1658	1.20±0.12	1.073	1.15±0.49	-0.302±0.030	-0.270	-0.29±0.12
-135°	1660	1.24±0.12	1.144	1.15±0.49	-0.312±0.030	-0.287	-0.29±0.12
-135°	1687	1.26±0.12	1.147	1.15±0.49	-0.315±0.030	-0.288	-0.29±0.12
155°	1696	1.20±0.12	1.099	1.15±0.49	-0.301±0.030	-0.276	-0.29±0.12
155°	1758	1.20±0.12	1.101	1.15±0.49	-0.301±0.030	-0.276	-0.29±0.12
-155°	1761	1.24±0.12	1.141	1.15±0.49	-0.312±0.030	-0.287	-0.29±0.12
-155°	1796	1.26±0.12	1.143	1.15±0.49	-0.316±0.030	-0.287	-0.29±0.12
-155°	1831	1.18±0.12	1.081	1.15±0.49	-0.295±0.030	-0.271	-0.29±0.12
-155°	2012	1.25±0.12	1.112	1.15±0.49	-0.312±0.030	-0.279	-0.29±0.12
-155°	2014	1.27±0.12	1.111	1.15±0.49	-0.318±0.030	-0.279	-0.29±0.12
-135°	2041	1.26±0.12	1.123	1.15±0.49	-0.315±0.030	-0.282	-0.29±0.12
-135°	2252	1.23±0.12	1.140	1.15±0.49	-0.309±0.030	-0.286	-0.29±0.12
-90°	2260	1.22±0.12	1.125	1.15±0.49	-0.307±0.030	-0.283	-0.29±0.12
-90°	2429	1.21±0.12	1.122	1.15±0.49	-0.304±0.030	-0.282	-0.29±0.12
-50°	2432	1.22±0.12	1.118	1.15±0.49	-0.305±0.030	-0.281	-0.29±0.12
-50°	2498	1.25±0.12	1.126	1.15±0.49	-0.315±0.030	-0.283	-0.29±0.12
0°	2500	1.24±0.12	1.097	1.15±0.49	-0.311±0.030	-0.276	-0.29±0.12
25°	2628	1.16±0.12	1.095	1.15±0.49	-0.292±0.030	-0.275	-0.29±0.12
	2688	1.93±0.15	1.922	1.82±0.48	-0.629±0.048	-0.628	-0.59±0.16
	2722	-	0.965	-	-	-1.478	-
50°	2838	0.640±0.118	0.720	0.84±0.49	-0.161±0.030	-0.181	-0.21±0.12
90°	3046	0.645±0.119	-	0.84±0.49	-0.162±0.030	-	-0.21±0.12
135°	3308	0.599±0.118	0.798	0.84±0.49	-0.150±0.030	-0.200	-0.21±0.12
135°	3311	0.569±0.118	0.798	0.84±0.49	-0.143±0.030	-0.200	-0.21±0.12
155°	3648	0.633±0.118	0.810	0.84±0.49	-0.159±0.030	-0.203	-0.21±0.12
180°	3936	0.680±0.118	0.828	0.84±0.49	-0.171±0.030	-0.208	-0.21±0.12
	4035	0.747±0.118	0.868	0.84±0.49	-0.187±0.030	-0.218	-0.21±0.12

Table 3: Electron arm spectrometer offsets (mm).

θ_{cm}	run	carbon x	LVDT x	survey x	carbon z	LVDT z	survey z
	1061	-0.248±0.250	-0.829	-0.74±0.34	-0.267±0.269	-0.892	-0.80±0.37
0°	1216	2.35±0.25	1.868	-	2.14±0.23	1.700	-
25°	1240	2.71±0.24	2.364	-	2.12±0.19	1.854	-
25°	1271	2.73±0.24	2.356	-	2.14±0.19	1.847	-
-25°	1273	-0.322±0.252	-0.618	-	-0.337±0.264	-0.648	-
-25°	1274	-0.232±0.252	-0.748	-	-0.243±0.263	-0.783	-
-25°	1310	-0.296±0.250	-0.761	-	-0.310±0.262	-0.797	-
50°	1311	2.94±0.23	2.835	-	2.01±0.16	1.932	-
50°	1390	3.18±0.24	2.818	-	2.17±0.16	1.902	-
-50°	1399	0.438±0.247	-0.306	-	0.525±0.296	-0.367	-
-50°	1420	0.436±0.248	-0.319	-	0.522±0.297	-0.382	-
-90°	1427	0.206±0.236	-0.449	-	0.292±0.335	-0.636	-
-90°	1459	0.204±0.237	-0.475	-	0.290±0.336	-0.673	-
90°	1467	3.18±0.22	3.222	-	1.82±0.13	1.845	-
90°	1547	3.20±0.22	3.201	-	1.84±0.12	1.833	-
135°	1562	2.49±0.22	2.603	-	1.49±0.13	1.551	-
135°	1658	2.45±0.22	2.681	-	1.46±0.13	1.598	-
-135°	1660	0.239±0.241	-0.288	-	0.325±0.327	-0.392	-
-135°	1687	0.260±0.240	-0.325	-	0.353±0.326	-0.441	-
155°	1696	2.81±0.24	2.779	-	1.95±0.17	1.925	-
155°	1758	2.71±0.24	2.797	-	1.88±0.16	1.938	-
-155°	1761	-0.018±0.248	-0.521	-0.53±0.32	-0.021±0.293	-0.616	-0.63±0.38
-155°	1796	-0.033±0.249	-0.589	-0.53±0.32	-0.039±0.293	-0.695	-0.63±0.38
-155°	1831	0.058±0.247	-0.601	-0.53±0.32	0.069±0.292	-0.710	-0.63±0.38
-155°	2012	0.094±0.248	-0.558	-0.53±0.32	0.111±0.292	-0.659	-0.63±0.38
-155°	2014	0.049±0.248	-0.564	-0.53±0.32	0.006±0.292	-0.666	-0.63±0.38
-135°	2041	0.630±0.240	0.002	-	0.855±0.325	0.003	-
-135°	2252	0.708±0.239	-0.019	-	0.962±0.325	-0.026	-
-90°	2260	0.575±0.237	-0.120	-	0.815±0.335	-0.170	-
-90°	2429	0.514±0.236	-0.145	-	0.728±0.335	-0.205	-
-50°	2432	2.35±0.25	1.572	-	2.82±0.30	1.884	-
-50°	2498	2.34±0.25	1.629	-	2.81±0.30	1.954	-
0°	2500	2.87±0.25	2.152	-	2.61±0.23	1.957	-
25°	2628	3.00±0.24	2.432	-	2.35±0.19	1.907	-
	2688	0.198±0.254	-0.326	-0.23±0.34	0.213±0.273	-0.351	-0.25±0.37
	2722	1.15±0.14	1.208	1.11±0.48	0.329±0.039	0.346	0.32±0.14
50°	2838	3.98±0.23	3.262	-	2.71±0.16	2.223	-
90°	3046	3.63±0.22	3.382	-	2.08±0.12	1.937	-
135°	3308	2.81±0.22	2.626	-	1.68±0.13	1.565	-
135°	3311	2.80±0.22	2.616	-	1.67±0.13	1.559	-
155°	3648	0.099±0.235	-0.265	-	0.068±0.162	-0.184	-
180°	3936	0.452±0.251	-0.210	-	0.411±0.228	-0.191	-
	4035	0.585±0.239	-0.361	-0.53±0.29	0.811±0.331	-0.500	-0.73±0.41

Table 4: Hadron arm spectrometer offsets (mm).

θ_{cm}	run	electron carbon	electron LVDT	hadron carbon	hadron LVDT	survey z_{tg}
	1061	1.001±0.032	0.876±0.032	0.958±0.046	-0.210±0.046	1.01±0.50
0°	1216	1.006±0.035	1.436±0.035	0.984±0.057	0.010±0.057	1.01±0.50
25°	1240	1.036±0.040	1.409±0.040	1.007±0.041	0.291±0.041	1.01±0.50
25°	1271	0.994±0.050	1.470±0.050	1.006±0.034	0.232±0.034	1.01±0.50
-25°	1273	1.020±0.076	1.351±0.076	0.989±0.069	0.364±0.069	1.01±0.50
-25°	1274	1.003±0.033	1.405±0.033	1.012±0.060	-0.021±0.060	1.01±0.50
-25°	1310	0.957±0.040	1.398±0.040	1.001±0.036	0.070±0.037	1.01±0.50
50°	1311	0.992±0.065	1.384±0.065	0.998±0.035	0.759±0.035	1.01±0.50
50°	1390	0.555±0.052	0.770±0.052	0.304±0.051	-0.482±0.051	0.46±0.50
-50°	1399	0.561±0.054	0.720±0.054	0.424±0.039	-1.089±0.039	0.46±0.50
-50°	1420	0.429±0.034	4.830±0.034	0.457±0.062	-1.070±0.062	0.46±0.50
-90°	1427	0.588±0.052	0.889±0.052	0.412±0.040	-0.976±0.040	0.46±0.50
-90°	1459	0.468±0.036	4.939±0.036	0.449±0.056	-0.980±0.056	0.46±0.50
90°	1467	0.489±0.065	0.917±0.065	0.390±0.051	0.479±0.051	0.46±0.50
90°	1547	0.455±0.044	0.879±0.044	0.429±0.058	0.424±0.058	0.46±0.50
135°	1562	0.434±0.062	0.878±0.062	0.344±0.064	0.595±0.064	0.46±0.50
135°	1658	0.478±0.056	1.031±0.055	0.452±0.070	0.982±0.070	0.46±0.50
-135°	1660	0.445±0.040	0.859±0.040	0.474±0.059	-0.609±0.060	0.46±0.50
-135°	1687	0.403±0.051	0.897±0.051	0.453±0.052	-0.768±0.052	0.46±0.50
155°	1696	0.460±0.045	0.888±0.045	0.451±0.088	0.405±0.088	0.46±0.50
155°	1758	0.456±0.043	0.873±0.043	0.442±0.081	0.598±0.081	0.46±0.50
-155°	1761	0.459±0.044	0.891±0.044	0.472±0.061	-0.550±0.061	0.46±0.50
-155°	1796	0.447±0.043	0.958±0.043	0.465±0.063	-0.686±0.064	0.46±0.50
-155°	1831	0.433±0.050	0.857±0.049	0.453±0.041	-0.883±0.041	0.46±0.50
-155°	2012	0.460±0.045	1.039±0.045	0.457±0.050	-0.869±0.050	0.46±0.50
-155°	2014	0.456±0.055	1.128±0.054	0.408±0.043	-0.782±0.043	0.46±0.50
-135°	2041	0.432±0.045	1.034±0.045	0.464±0.041	-0.846±0.041	0.46±0.50
-135°	2252	0.456±0.043	0.845±0.043	0.471±0.039	-1.056±0.039	0.46±0.50
-90°	2260	0.471±0.034	0.881±0.034	0.471±0.045	-1.004±0.045	0.46±0.50
-90°	2429	0.457±0.055	0.846±0.055	0.452±0.040	-0.955±0.041	0.46±0.50
-50°	2432	0.444±0.049	0.875±0.049	0.435±0.051	-1.146±0.051	0.46±0.50
-50°	2498	0.486±0.040	1.023±0.040	0.413±0.064	-1.021±0.065	0.46±0.50
0°	2500	0.427±0.041	1.064±0.041	0.400±0.066	-1.021±0.067	0.46±0.50
25°	2628	0.439±0.034	0.714±0.034	0.426±0.049	-0.747±0.049	0.46±0.50
	2688	0.441±0.052	0.453±0.052	0.330±0.101	-0.677±0.102	0.46±0.50
	2722	-	-	0.987±0.129	1.086±0.111	1.14±0.50
50°	2838	1.127±0.039	0.785±0.039	1.139±0.048	-0.420±0.048	1.14±0.50
90°	3046	1.138±0.054	-	1.135±0.042	0.556±0.042	1.14±0.50
135°	3308	1.106±0.046	0.267±0.046	1.119±0.056	0.714±0.056	1.14±0.50
135°	3311	1.152±0.047	0.160±0.047	1.118±0.055	0.700±0.055	1.14±0.50
155°	3648	1.114±0.042	0.352±0.042	1.131±0.068	0.342±0.067	1.14±0.50
180°	3936	1.150±0.045	0.509±0.044	1.145±0.059	-0.177±0.058	1.14±0.50
	4035	1.147±0.038	0.616±0.038	1.124±0.053	-0.870±0.054	1.14±0.50

Table 5: Electron and hadron arm *reactz* positions and survey z_{tg} (mm).